

# Journal of Engineering Technology and Applied Physics

## SCS+C Topographic Correction to Enhance SVM Classification Accuracy

Jwan AL-Doski<sup>1,\*</sup>, Shattri B. Mansor<sup>2</sup>, H'ng Paik San<sup>3</sup> and Zailani Khuzaimah<sup>4</sup>

<sup>1,2,4</sup>Civil Department, Faculty of Engineering, Universiti Putra Malaysia, Serdang, Selangor, Malaysia.

<sup>3</sup>Forest Production Department, Faculty of Forestry, Universiti Putra Malaysia, Serdang, Selangor, Malaysia.

\*Aldoski-Jwan@hotmail.com, shattri@gmail.com, ngpaiksan@upm.edu.my, zailanikhuzaimah@gmail.com

<https://doi.org/10.33093/jetap.2020.x1.7>

**Abstract** – The topographic impact may change the radiance values captured by the spacecraft sensors, resulting in distinct reflectance value for similar land cover classes and mischaracterization. The problem can be more clearly seen in rugged terrain landscapes than in flat terrains, such as the mountainous areas. In order to minimize topographic impacts, we suggested the implementation of Modified Sun-Canopy-Sensor Correction (SCS+C) technique to generate land cover maps in Gua Musang district which is located in a rugged mountainous terrain area in Kelantan state, Malaysia using an atmospherically corrected Landsat 8 imagery captured on 22 April 2014 by Support Vector Machine (SVM) algorithm. The results showed that the SCS+C method reduces the topographic effect particularly in such a steep and forested terrain with classification accuracy improvement about 4 % which was statistically significantly with the McNemar test value Z and P measured 6.42 and 0.0001 on the corrected image classification 90.1 % accuracy compared to the uncorrected image 86.2 % for the test area. Thus, the topographic correction is suggested to be the main step of the data pre-processing stage in mountainous terrain before SVM image classification.

**Keywords**—Support Vector Machine, modified Sun-Canopy-Sensor Correction (SCS+C) Technique, land cover, landsat 8 imagery

### I. INTRODUCTION

Deforestation is a very broad concept, consisting of cutting trees including frequent lopping, felling, and forest litter removal, walking, grazing, and seedling trampling. It can also be described as removing or damaging the vegetation in a forest insofar as it no longer sustains its natural flora and fauna [1]. When the research region is positioned in rough or mountainous areas, the significant part of pre-processing is a topographic correction. Varied terrain orientation frequently leads to land pixel signal values to vary. Topographic correction is indeed essential in order to quantitatively analyze the remote sensing image until the classification phase typically in these area [2]. There are many topographical

correction empirical and non-empirical parametric models have been extensively used it to suppress topographical consequences on remote sensing data, the common methods applied C, SCS+C and Minnaert techniques [3]. The superior output of semi-empirical corrections, including C and empirical-statistical corrections, and Minnaert correction is noticeable in several of these researches.

Number of studies have shown that adjustment of topographical consequences performed prior to the use of multispectral and multi-temporal pixel classification can significantly enhance classification accuracy, especially if the location of the research is in rough terrain [4]. For example, [5] discovered that by combining atmospheric and slope-like correction, the forest to-non-forest classification accuracy of nearly 90 % in mountainous pre-Alps in central Switzerland could also be accomplished with the help of high-quality ground truth. They also discovered that atmospheric correction alone did not substantially enhance the classification opposed to utilizing only a correction of the slope and aspect. [6], assessed the topographical correction techniques for improving soil cover mapping using object-based Landsat 5 TM image. The C, SCS+C and Minnaert techniques showed the best output, followed by S2 and E-Stat, with an overall accuracy rise of around 10 %. Land cover classification varied in a big part of the complete region studied from uncorrected and corrected data, with values of about 29 % for all correction techniques.

References [7] and [8] a topographically corrected imagery was implemented to the SVM classifier, achieving appropriate accuracy. The findings indicate that after topographic correction, the precision of the classification of land cover improved. Of Landsat TM-5 and OLI-8 information, particular accuracy rises ranged from 3 % to 3.97 %, to 0.44 % and 1.34 %, with Kappa coefficient rises of 2.4 % – 4.9 % and 1.6 % – 2.9 %, respectively. In other study, [9], the accuracy of the land cover was evaluated and opposed for the four scenarios. The topographically uncorrected LC

classification led in overall accuracies of 78 % (1985), 79 % (1995) and 84 % (2010), respectively. The topographic correction enhanced the classification of ML with 3 % (1985), 3 % (1995) and 2 % (2010) respectively. The classification of SVM was also carried out on topographically uncorrected and corrected composites. The overall accuracy of the topographically uncorrected SVM classification was 83 % (1985), 83 % (1995) and 89 % (2010), respectively. The revised classification of SVM led in an increase in overall classification accuracies of 2 % (1985), 0 % (1995) and 2 % (2010) respectively. Typically, for all years, the overall accuracies for LC courses were between 78 % and 91 %.

Multiple writers contrasted the MLC for the most effective topographical correction techniques and recorded an increase in the overall accuracy of 1 %-10 % [7, 8] in other studies like [10] by an overall accuracy up to 40 %. In some cases, however, the correction did not improve the classification accuracy satisfactorily [11, 12]. Topographic and atmospheric correction models are diverse and the choice of one model relies on its effectiveness to decrease the relief impact and ease of application and on the performance and study region of remote sensing data. Although, it is pointless to compare the studies since the input files and parameters are different and depend on in study areas, vegetation types, sensors, and DEM, atmospheric and topographic corrections methods. Furthermore, the adjusted SCS correction technique is suitable for mapping regions of forest land cover [13, 14]

We concentrated on topographic impacts on land cover mapping precision in this paper, and in the previous paragraph, we highlight associated work on topographic impacts to improve land cover mapping accuracy. In order to minimize topographic impacts, we suggested the implementation of Modified Sun-Canopy-Sensor Correction (SCS+C) technique to generate land cover maps in Gua Musang district which is located in a rugged mountainous terrain area in Kelantan state, Malaysia using an atmospherically corrected Landsat 8 imagery by Support Vector Machine (SVM) algorithm.

## II. STUDY AREA (GUA MUSANG)

Gua Musang is a southern Kelantan, Malaysia, district and parliamentary constituency. It's Kelantan's biggest district. It is administered by the district council of Gua Musang and bordered on the south by the state of Pahang, on the east by Terengganu, on the west by Perak and on the north by Kuala Krai and Jeli districts of Kelantan. It is about 140 km south of the government capital Kota Bharu, a tiny railway town. The study area included Gua Musang in northwestern Malaysia, which is encompassed within 4° 53' 3.4044" N and 101° 58' 5.4408" E, covering an area of 4600 km<sup>2</sup> (Fig. 1). The countryside is rough with a broad altitude (121–1770 m above sea level), and topographically classified into three kinds: mountains (> 500 m above sea level), hills (200–500 m above sea level) and valleys (< 200 m above sea level). The elevation of terrain reduces from northwest to southeast, and about 35 percent of the study region accounts for mountainous terrain. The primary LC is woodland, which for food production was mainly cleared before the 1990s but has now been reforested in reaction to public measures. Other types of land cover include food plants like oil palm and rubber [15, 16].

## III. METHODOLOGY

The methodology is shown in Fig. 2. The uncorrected (UI) and corrected (CI) image were developed by applying SVM classification on both images.

### A. Data Source and Pre-processing

Landsat 8 OLI (30 m) was used for LC mapping on 22 April 2014 and was received from the site of the earth explorer (<http://earthexplorer.usgs.gov/>). This data set was imported in ENVI 5.1v Software and preprocessed including geometric and atmospheric corrections prior to topographic correction. Nevertheless and, this image includes digital number (DN) matrices with 55,000 gray levels, the image data must be based on reflectance values, and thus it is essential to convert the DNs to reflectance which done by two steps. First, the OLI data was transformed into ENVI image file, the file contained wavelength details, bands, DN transformation into reflectance. Using the spectral radiance scaling factor in the OLI metadata file, Eq. (1) was used to convert DN values to spectral radiance.

$$L\lambda = ML * Q_{cal} + AL \quad (1)$$

where the radiance ( $W/m^2 \cdot sr \cdot \mu m$ ) is  $L\lambda$ , the multiplicative scaling factor for each band is ML, the pixel value in DN for level 1 is  $Q_{cal}$ , and the additive scaling factor for each band is AL. The image was then saved and converted to the bit in line intelligence format. Second, for this purpose Radiance to Reflectance Conversion, the FLAASH method has been used to transform radiance values to the top of atmospheric correction (TOA).

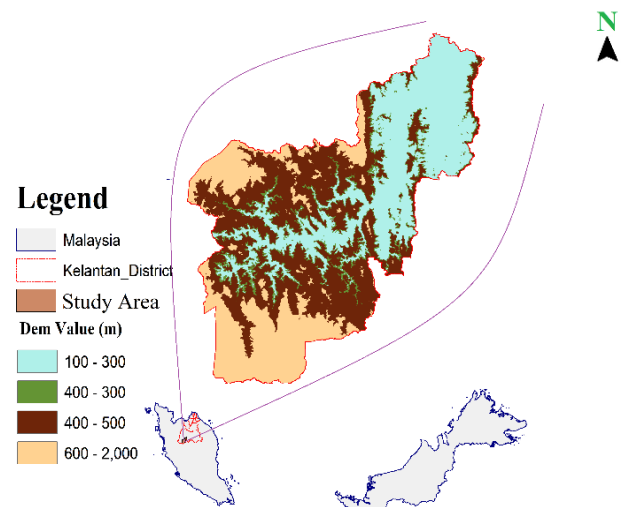


Fig. 1. Location of Gua Musang, Malaysia.

The image was further saved and a single scale factor value (1000) was applied to all bands for transform [ $(Wm^2 \mu m sr) * 100$ ] input radiance image into normal FLAASH input units ( $\mu W / cm^2 nm sr$ ). Reflectance values in FLAASH image were multiplied by 10,000 so the resulting value ranged from 0 to 1. Equation (2) has been used to directly transform DN values to TOA reflectance.

$$\rho^* \lambda = M\rho * Q_{cal} + A\rho \quad (2)$$

where the spectral reflectance (unitless) without correction of solar angle is  $\rho^* \lambda$ , the multiplicative scaling factor for each band is  $M\rho$ , the pixel value in DN (level 1) is  $Q_{cal}$ , and the additive scaling factor for each band is  $A\rho$ . Equation (3) has been used to transform TOA reflectance with solar angle.

$$\rho\lambda = \rho'\lambda \cdot \sin(\theta) \quad (3)$$

where the TOA reflectance (unitless) is  $\rho\lambda$  and the solar elevation angle is  $\theta$ . The next stage is the correction of geometrics. With 24 uniformly distributed GCPs, the Landsat 8 data was geometrically projected onto the SPOT 5 image register using a bilinear conversion, the re-registration was carried out with an accuracy of 0.5 pixels.

**B. False Color Composite (FCC)**

A layer stack option has been implemented in the image interpreter tool box to generate an FCC. For the extraction of study region, the sub-setting tool of satellite image was conducted by taking Gua Musang's geo-referenced line border as AOI (Area of Interest). Some indices such as the normalized difference vegetation index (NDVI), the Soil Adjusted Vegetation Index (SAVI) and the Simple Ratio (SR) have also been developed to classify Landsat 8 images (Fig. 3) for better classification outcomes.

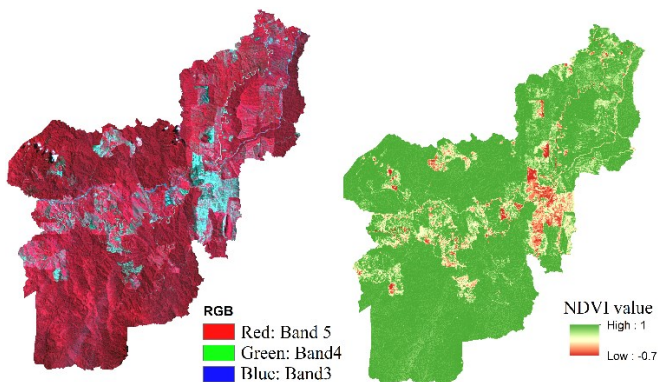


Fig. 3. The landsat 8 image of Gua Musang in FCC color and NDVI image.

**C. DEM Generation**

The DEM layer used in this research is the SRTM at 1 arc sec (approx. 30 m x 30 m) resolution levels with Z precisions usually among 10 m and 25 m Mean Root Square Error. It was generated in 2011 from stereo-pair images acquired with nadir and backward images of ASTER over the same area. The exact date of acquisition of ASTER stereo-pair data was not available.

**D. Topographic Correction (TC)**

After the at-satellite radiances were directly converted to at-surface reflection, SCS+C as TC method was performed to develop the CI image using Eqs (3) and (4) [14]. On the other hand, no TC was applied on the development of the UI image.

$$p_{H,\lambda} = p_{T,\lambda} \frac{\cos \theta_t \cos \theta_s + C_\lambda}{\cos i + C_\lambda} \quad (4)$$

With  $\cos i = \cos \theta_s \cos \theta_t + \sin \theta_s \sin \theta_t \cos(\phi_s - \phi_t)$

$P_{H,\lambda}$  (the normalized reflectance);  $i$  (the solar incident angle);  $\theta_t$  (the slope angle);  $\theta_s$  (the solar zenith angle);  $\phi_s$  (the solar azimuth angle);  $\phi_t$  (the aspect angle);  $C_\lambda$  (empirical parameters ( $c=b/m$ )),  $c$  (a function of the regression slope ( $b$ ) and intercept ( $m$ )), which was acquired using regression between  $\cos i$  and  $P_{H,\lambda}$  800 sample points were assigned in different terrain and illumination condition to derive  $\cos i$  value.

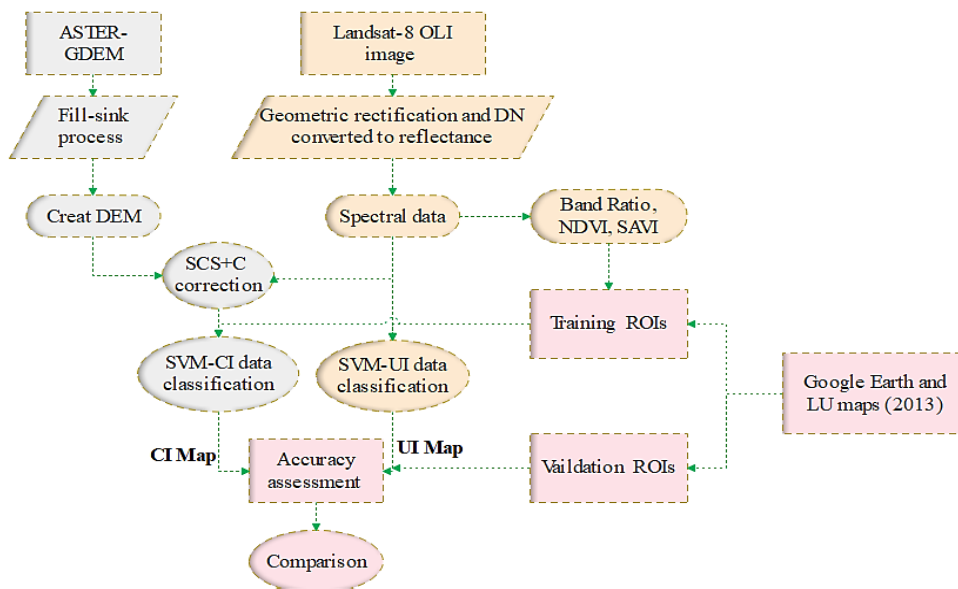


Fig. 2. The study methodology for SVM improving using SCS+C.

**E. RBF-Based SVM Classification and Evaluation**

The classification system by [17] is proposed. Table I presents descriptions of the nine classes in this system. Training data samples is the crucial step in a supervised classification method like SVM. Training data were randomly chosen from comparatively homogeneous areas of the

research region corresponding to the chosen land cover classes using the ROI instruments supplied by ENVI software (v. 5.1) with the assistance of ground expertise, land cover and forest type cover maps acquired from the Ministry of Agriculture and Forestry, Malaysia for 2013 and the Google Earth tool. 100 pixels for each land cover were equally selected as validation samples for image classification

accuracy assessment. For assessing quality of training data, the measurement of J – M is based on distance from Bhattacharya. It enables to show how statistically distinct a chosen spectral class pair is. J – M distance is provided using Eq. (5) for two classes a and b;

$$JM_{ab} = \sqrt{2(1 - \exp(-\alpha))}$$

$$\alpha = \frac{1}{8}(\mu_a - \mu_b)^T \left(\frac{C_a + C_b}{2}\right)^{-1}(\mu_a - \mu_b) + \frac{1}{2} \ln \left[ \frac{\frac{1}{2}|c_a + c_b|}{\sqrt{|c_a||c_b|}} \right] \quad (5)$$

where the mean values are  $\mu_a$  and  $\mu_b$  for categories a and b, the covariance matrices for categories a and b are  $C_a$  and  $C_b$  and the vector denotes J – M distance range is an index of 0.0 to 2.0. Its > 1.7 values show the classes are well segregated. A J – M distance value < 1.0 shows bad class separability. The separability for selected training sites of all classes in this study were examined by computing their spectral separability, and the J–M distance values were measured between land cover classes range from 1.7 to 2. For CI and UI classification, SVM base on RBF was applied. The outcomes of the SVM-based RBF kernel seemed to have least computing problems, the penalty value C and the kernel parameter  $\pi$  were the two specifications used for the RBF kernel, the  $\gamma$  was calculated as the inverse of the OLI ortho imagery number of spectral bands and a value of 0.167 was assigned. The maximum value (100) of the C has been allocated. A zero value was allocated to the pyramid parameter, and a zero was allocated to the probability limit as set as suggested in the ENVI User Manual. Eq. (6) demonstrates the internal function type of the RBF product.

$$K(x, y) = \exp \left\{ -\frac{|x-y|^2}{2\sigma^2} \right\} \quad (6)$$

where x and y are depicted as function vectors in certain input areas, and  $\sigma$  is the variance.

Table I. Summary of training (ROIS) areas used for modification SCS+C AS TC method.

No.	Land Cover Classes	Description	Training
1	Forests	Primary and secondary forests: tall dense trees and Planted trees	2149
2	Water Bodies	The Areas covered either by river beds or by man-made earth dams, dams filled with sand, streams, lakes, reservoirs and ponds.	1539
3	Oil Palm	areas with oil palm trees	2225
4	Rubber	areas with rubber trees	718
5	Crop Land	The Land used primarily for the production of food plants such as maize, green grams, beans, cassava and mangos. The cultivation of crops in this territory is either irrigated or rainfed	238
6	Grass Land	This class of LC defines grass as the main vegetation cover	538
7	Barren Land	This describes the land left without vegetation cover	1696
8	Built-Up Area	The LC with the rural and urban building. It involves infrastructure for commercial, residential, industrial and transportation.	590
9	Others	Not given in the categories from 1 to 9	845
Total Pixels Used			10538

F. Performance Accuracy Assessment

The criteria for assessing classification algorithms efficiency include accuracy, speed, stability and comprehensibility [18]. The aim of the assessment relies on

which criterion or group of criteria to be used. As the most appropriate criterion for all directions and for all reasons. In this evaluation, accuracy, speed and stability were chosen as criterion. In standings of producer accuracy (PA), user accuracy (UA), and overall accuracy (OA), an error matrix was produced to provide a means of expressing every class accuracy and their contribution to OA. Kappa coefficient (k) was frequently used to estimate how much better a specific classification relative to a random classification and to determine a confidence interval to equate two or even more classifications statistically. The OA, PA, UA and K were calculated as:

$$UA = \frac{n_{ii}}{n_{irow}}, \quad OA = \frac{1}{N} \sum_{i=1}^r n_{ii},$$

$$K_c = N \sum_{i=1}^r n_{ii} - \sum_{i=1}^r \frac{n_{icol} n_{irow}}{N^2} - \sum_{i=1}^r n_{icol} n_{irow}, \quad PA = \frac{n_{ii}}{n_{icol}},$$

where  $n_{ii}$  is the number of pixels in a category properly categorized; N is the overall number of pixels throughout the confusion matrix; r is the rows number; and  $n_{icol}$  and  $n_{irow}$  are total columns (reference data) and rows (expected classes). Among the most commonly used techniques of comparing accuracies is comparing two autonomous kappa values. It is possible to evaluate the statistical significance of the distinction between the two values by calculating a Z value. There are, indeed, several problems concerning the quality of the kappa interpretation. Expressing accuracies as the percentage of properly assigned pixels (i.e., general precision) is therefore preferable, as described in [19]. For all the classifications, the same set of reference samples was used in this study. Thereby, for all the techniques adhered, each set of reference samples could be preserved as dependent samples. In such a scenario, the meaning of the difference between the two percentages (overall accuracy) was assessed using Eq. (7) for the McNemar test [20, 21].

$$Z = \frac{f_{12} - f_{21}}{\sqrt{f_{12} + f_{21}}} \quad (7)$$

where the validation data frequency at row i column j is  $f_{ij}$ . The number of pixels of one technique properly categorized as opposed to the number of pixels of another technique wrongly categorized are  $f_{12}$  and  $f_{21}$ . The classified images from SVM were evaluated using the error matrix statistics calculation as well as K analysis was also conducted to assess whether there were two considerably distinct classifications

IV. RESULTS AND DISCUSSION

Figures 4 and 5 show the comparison of Landsat 8 OLI and RBF-based SVM classification results from the UI and CI. Topographic effects are clearly seen in the rugged terrain in the UI. The slope facing off the illumination source in the CI appears brighter than the same path in the UI as a consequence of TC. (Figs. 4 (a) and (b)). In both tables (II and III) demonstrate UI and CI classification process accuracy (OA). The OA for the Landsat 8 OLI imagery increase from 86.22 % to 90.11 %, after TC being performed. Generally, forest classes have low accuracies for the UI due to the topographic effect. Most of the forests are placed in rugged terrain, which contributes to the different illumination of slopes. Different reflectance values of forest trees communities result in the two classes could be separated in

different classes. However, cloud shadows which are mainly located in the mountainous area in test area altered the actual DN, thus prompted the misclassification of the forest, oil palm and rubber. Compared to the CI classification, this also influenced the reduced UI image classification OA. The McNemar test value Z and P measured between corrected image (with SCS+C) and un-corrected image (with SCS+C) by SVM classifier about 6.42 and 0.0001 which mean the corrected image by SVM thus had a substantial benefit over un-corrected image by SVM because the McNemar test value of the McNemar is higher than 1.96, the first technique offers a statistically significant ( $p \leq 0.05$ ) enhancement in the outcomes of the classification.

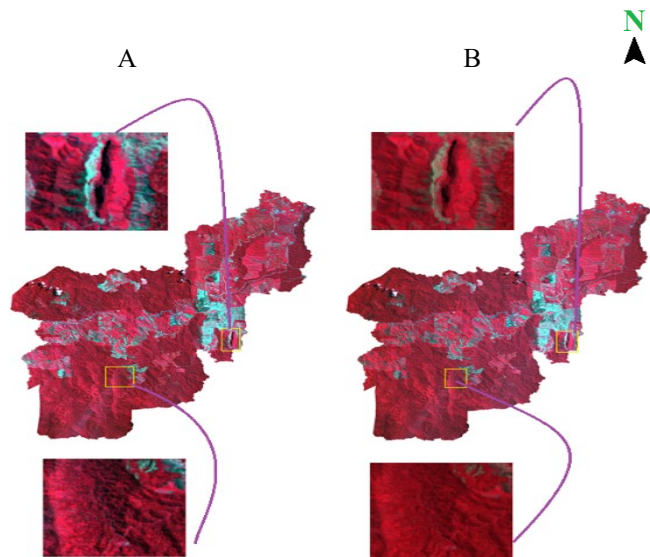


Fig. 4. The uncorrected (A) and corrected (B) infrared images of the test area.

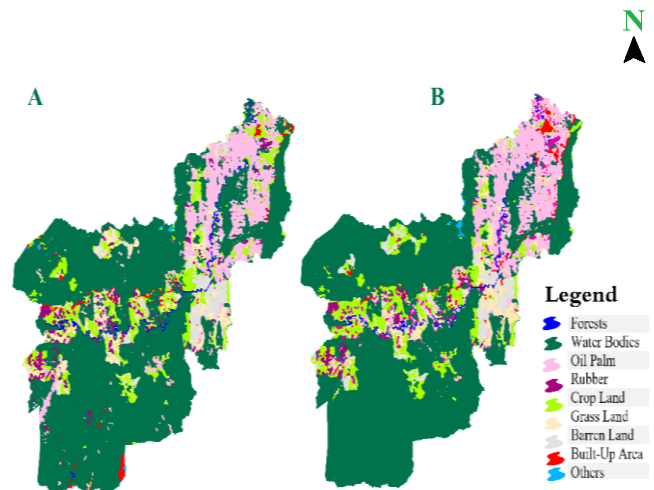


Fig. 5. The RBF-based SVM classification results from the uncorrected TC (A) and corrected TC images (B).

A similar increase in accuracy for image classification through the application of the SCS+C method was also achieved in a study conducted in Kheyroud Kenar forest in Iran [22]. The research showed that the TC was able to enhance accuracy from 75.22 % to 82.13 %. In other study [4] land cover mappings in Ci Kapundung and Ci Sangkuy upper catchment areas on rough terrain in Bandung Basin, Indonesia, images were acquired from Spot 6 and classified using object-based satellite image classification. Under these circumstances, the topographic correction technique was selected as a modified sun-canopy-sensor correction (SCS+C). Based on the OA, its performance was assessed. Result indicates that the correction technique could enhance the accuracy of the first and second case studies to 77 % and 87.58 % respectively [4].

Table II. Accuracy assessment for uncorrected image (without SCS+C) as topographic correction).

Land Cover Classes	Water Bodies	Forests	Oil Palm	Rubber	Crop Land	Grass Land	Barren Land	Built-Up Area	Others	Total	PA %	UA %
Water Bodies	63	0	0	0	0	1	4	3	0	71	63	88.73
Forests	13	100	4	21	10	0	0	1	0	149	100	67.11
Oil Palm	7	0	96	3	0	0	1	2	0	109	96	88.07
Rubber	0	0	0	76	0	0	0	0	0	76	76	100
Crop Land	0	0	0	0	89	0	0	3	0	92	89	96.74
Grass Land	3	0	0	0	1	94	2	0	0	100	94	94
Barren Land	2	0	0	0	0	0	91	15	0	108	91	84.26
Built-Up Area	12	0	0	0	0	5	2	76	0	95	76	80
Others	0	0	0	0	0	0	0	0	100	100	100	100
Total	100	100	100	100	100	100	100	100	100	900		
OVA	86.22%											
KAPPA	0.85											

Table III. Accuracy assessment for corrected image (with (SCS+C) as topographic correction).

Land Cover Classes	Water Bodies	Forests	Oil Palm	Rubber	Crop Land	Grass Land	Barren Land	Built-Up Area	Others	Total	PA%	UA%
Water Bodies	98	0	0	0	0	0	0	0	0	98	98	100
Forests	2	82	9	0	1	0	0	0	0	91	82	86.81
Oil Palm	0	5	89	2	0	8	0	0	0	103	89	85.44
Rubber	0	0	2	93	0	3	0	0	0	97	93	95.88
Crop Land	0	3	0	0	96	1	7	2	0	109	96	88.07
Grass Land	0	6	0	1	3	79	12	0	0	101	79	78.22
Barren Land	0	2	0	0	0	9	65	0	0	76	65	85.53
Built-Up Area	0	2	0	4	0	0	16	96	0	114	96	84.21
Others	0	0	0	0	0	0	0	2	100	102	100	98.04
Total	100	100	100	100	100	100	100	100	100	891		
OVA	90.11%											
KAPPA	0.88											

## V. SUMMARY

This paper proposes an evaluation effect of SCS+C as TC method on the RBF-based SVM classification performance using Landsat 8 imagery. The study showed that SCS+C method could significantly reduce the topographic effect on mapping accuracy particularly in such a steep and forested terrain. On the corrected image, there is an enhancement in classification accuracy relative to the uncorrected image for the test region from 86.22 % to 90.11 %. The McNemar test value Z and P measured statistically significant ( $p \leq 0.05$ ) between the corrected and un-corrected images by SVM classifier about 6.42 and 0.0001. To improve the RBF-based SVM image classification technique accuracy, atmospheric correction and the topographic correction are suggested being implemented for such mountainous and forested terrain before applying RBF-based SVM classification.

## ACKNOWLEDGEMENTS

Authors wish to gratefully acknowledge Prof. Shattri B. Mansor, Director of Remote Sensing and GIS Research Centre at Universiti Putra Malaysia, and Dr. Zailani Khuzaimah for the financial support, recommendations and guidance through this study. The authors wish to acknowledge the helpful comments and advice from both anonymous reviewers

## REFERENCES

- [1] P. Van Der Molen and D. Mitchell, "Climate Change, Land Use and Land Surveyors," *Survey Review*, vol. 48, no. 347, pp. 148-155, 2016.
- [2] A. Fahsi, T. Tsegaye, W. Tadesse and T. Coleman, "Incorporation of Digital Elevation Models with Landsat-TM Data To Improve Land Cover Classification Accuracy," *Forest Ecology and Management*, vol. 128, no. 1-2, pp. 57-64, 2000.
- [3] S. Vanonckelen, S. Lhermitte and A. Van Rompaey, "The Effect of Atmospheric and Topographic Correction Methods on Land Cover Classification Accuracy," *International Journal of Applied Earth Observation and Geoinformation*, vol. 24, pp. 9-21, 2013.
- [4] M. S. Rani, O. Schroth, R. Cameron and E. Lange, "The Effect of Topographic Correction on SPOT6 Land Cover Classification in Water Catchment Areas in Bandung Basin, Indonesia," in *GISRUK 2017 Proceedings*, 2017, no. 96: Geographical Information Science Research UK.
- [5] K. I. Itten and P. Meyer, "Geometric and Radiometric Correction of TM Data of Mountainous Forested Areas," *IEEE Transactions on Geoscience and Remote Sensing*, vol. 31, no. 4, pp. 764-770, 1993.
- [6] E. P. Moreira and M. M. Valeriano, "Application and Evaluation of Topographic Correction Methods to Improve Land Cover Mapping Using Object-Based Classification," *International Journal of Applied Earth Observation and Geoinformation*, vol. 32, pp. 208-217, 2014.
- [7] B. Tan et al., "Improved Forest Change Detection With Terrain Illumination Corrected Landsat Images," *Remote Sensing of Environment*, vol. 136, pp. 469-483, 2013.
- [8] S. Vanonckelen, S. Lhermitte and A. Van Rompaey, "The Effect of Atmospheric and Topographic Correction on Pixel-Based Image Composites: Improved Forest Cover Detection in Mountain Environments," *International Journal of Applied Earth Observation and Geoinformation*, vol. 35, pp. 320-328, 2015.
- [9] S. Vanonckelen, S. Lhermitte, V. Balthazar and A. Van Rompaey, "Performance of Atmospheric and Topographic Correction Methods on Landsat Imagery in Mountain Areas," *International Journal of Remote Sensing*, vol. 35, no. 13, pp. 4952-4972, 2014.
- [10] I. Gitas and B. Devereux, "The Role of Topographic Correction in Mapping Recently Burned Mediterranean Forest Areas from LANDSAT TM Images," *International Journal of Remote Sensing*, vol. 27, no. 1, pp. 41-54, 2006.
- [11] L. Blesius and F. Weirich, "The Use of The Minnaert Correction For Land-Cover Classification in Mountainous Terrain," *International Journal of Remote Sensing*, vol. 26, no. 17, pp. 3831-3851, 2005.
- [12] Z. Zhang, R. R. De Wulf, F. M. Van Coillie, L. P. Verbeke, E. M. De Clercq and X. Ou, "Influence of Different Topographic Correction Strategies on mountain vegetation classification accuracy in The Lancang Watershed, China," *Journal of Applied Remote Sensing*, vol. 5, no. 1, pp. 053512, 2011.
- [13] S. Soenen, D. Peddle, C. Coburn, R. Hall and F. Hall, "Improved Topographic Correction of forest image data using a 3-D Canopy Reflectance Model in Multiple Forward Mode," *International Journal of Remote Sensing*, vol. 29, no. 4, pp. 1007-1027, 2008.
- [14] S. A. Soenen, D. R. Peddle and C. A. Coburn, "SCS+ C: A Modified Sun-Canopy-Sensor Topographic Correction in Forested Terrain," *IEEE Transactions on Geoscience and Remote Sensing*, vol. 43, no. 9, pp. 2148-2159, 2005.
- [15] M. Hossain, J. Bujang, M. Zakaria and M. Hashim, "Application of Landsat Images to Seagrass Areal Cover Change Analysis for Lawas, Terengganu and Kelantan of Malaysia," *Continental Shelf Research*, vol. 110, pp. 124-148, 2015.
- [16] B. Satyanarayana, K. A. Mohamad, I. F. Idris, M. L. Husain and F. Dahdouh-Guebas, "Assessment of Mangrove Vegetation Based on Remote Sensing and Ground-Truth Measurements at Tumpat, Kelantan Delta, East Coast of Peninsular Malaysia," *International Journal of Remote Sensing*, vol. 32, no. 6, pp. 1635-1650, 2011.
- [17] J. R. Anderson, *A Land Use and land cover classification system for Use with Remote Sensor Data*. US Government Printing Office, 1976.
- [18] V. N. Mishra, R. Prasad, P. K. Rai, A. K. Vishwakarma and A. Arora, "Performance Evaluation of Textural Features in Improving Land Use/Land Cover Classification Accuracy of Heterogeneous Landscape Using Multi-Sensor Remote Sensing Data," *Earth Science Informatics*, vol. 12, no. 1, pp. 71-86, 2019.
- [19] G. M. Foody, "Status of Land Cover Classification Accuracy Assessment," *Remote Sensing of Environment*, vol. 80, no. 1, pp. 185-201, 2002.
- [20] G. M. Foody, "Thematic Map Comparison," *Photogrammetric Engineering & Remote Sensing*, vol. 70, no. 5, pp. 627-633, 2004.
- [21] P. Kumar, R. Prasad, A. Choudhary, V. N. Mishra, D. K. Gupta and P. K. Srivastava, "A Statistical Significance of Differences in Classification Accuracy of Crop Types Using Different Classification Algorithms," *Geocarto International*, vol. 32, no. 2, pp. 206-224, 2017.
- [22] N. Ghasemi, A. Mohammadzadeh and M. R. Sahebi, "Assessment of different topographic correction methods in ALOS AVNIR-2 Data Over A Forest Area," *International Journal of Digital Earth*, vol. 6, no. 5, pp. 504-520, 2013.

